Quantum Receiver for Binary Coherent-State Signals with Constant-Intensity Local Lasers

Victor A. Vilnrotter, *Senior Member, IEEE*

Abstract **– A quantum receiver capable of approaching the fundamental quantum limit on bit error probability is described and evaluated. Conventional optical and abstract quantum mechanical descriptions are provided and the underlying principles derived in both domains, thus providing a bridge to optimum quantum measurements in terms of well-understood optical communications concepts. Receiver performance is evaluated for the case of binary phase-shift keyed modulation, and it is shown that significant gains can be achieved over near-optimum receivers reported previously in the literature. This new receiver concept can be implemented using practical measurements amenable to high data-rate operation, hence it may enable future deep-space optical communications with performance approaching the greatest possible fidelity allowed by the laws of quantum mechanics.**

Index Terms **– Quantum detection, binary coherent-state signals, Helstrom bound.** [1]

I. Introduction

Deep-space optical communication is a key component of the NASA roadmap, with the goal of returning greater data-volumes from Mars and other solar-system encounters in future missions. Conventional optical receivers currently under consideration for deep-space communications employ photon-counting or coherent detection to potentially extract useful information even from a single photon, on the average. However, quantum mechanics promises greater gains, but fails to specify how these theoretical gains can be achieved in practice. When pure states are used to communicate information, such as those obtained from pulsed or phase-modulated lasers, the minimum achievable error probability subject to the laws of quantum mechanics has been determined by C. Helstrom [1], and hence referred to as the "Helstrom bound". So far, only a few schemes have been devised that are capable of achieving the Helstrom bound for a general class of binary signals, including: the Dolinar receiver [1] and the Sasaki-Hirota receiver [2]. The Dolinar receiver was the first structured approach that achieved the Helstrom bound using physically realizable measurements together with real-time optical feedback, however practical implementation at high data-rates was found to be challenging due to the requirement for precise local laser intensity control [3, 4]. A different approach was proposed by Sasaki and Hirota [2], which does not employ optical feedback but achieves the Helstrom bound via unitary transformations and photon counting. However, a practical implementation of the Sasaki-Hirota receiver requires multiphoton nonlinear optical processing, which also leads to complex receiver structures. The receiver structure proposed here overcomes these practical impediments by approaching the Helstrom bound using well-known practical measurements that enable high-speed implementation, while attaining significantly better performance than photon-counting, coherent detection or even near-optimum quantum receivers such as the "Kennedy receiver" which is exponentially optimum and implementable at high data-rates [1, 3, 4].

Manuscript submitted August 11th, 2012, revised November 19th 2012.
Author is with the Jet Propulsion Laboratory, California Institute of Technology, Pasadena, CA, 91109, USA (Victor.A.Vilnrotter@jpl.nasa.gov).

II. Quantum Description of Communications Signals

At any instant of time, the state of a quantum system is completely specified by a state vector $|\psi\rangle$ in a Hilbert space over the field of complex numbers. The state vector, or "ket" $|\psi\rangle$, can be thought of as a column vector of infinite dimensions. An equivalent "row vector" representation of the state vector is denoted by $\langle\psi|$ in Dirac notation.

If $|\psi_1\rangle$ and $|\psi_2\rangle$ are states of a quantum system, then so is their linear combination $|\psi\rangle = a_1|\psi_1\rangle + a_2|\psi_2\rangle$ where a_1 and a_2 are complex numbers. The row-vector representation is $\langle\psi| = a_1^*\langle\psi_1| + a_2^*\langle\psi_2|$. The "overlap" between two states $|\psi\rangle$ and $|\varphi\rangle$ is the complex number $\langle\psi|\varphi\rangle$ or its complex conjugate $\langle\varphi|\psi\rangle$. If the overlap is zero, the states are orthogonal. The state is normalized if $\langle\psi|\psi\rangle = 1$. Thus, for orthonormal states $\langle\psi_m|\psi_n\rangle = \delta_{mn}$, where δ_{mn} is the Kroenecker delta. If $|\psi_1\rangle$ and $|\psi_2\rangle$ are orthonormal and $|\psi\rangle$ is normalized, then their overlap is

$$\begin{aligned}\langle\psi_1|\psi\rangle &= \langle\psi|\psi_1\rangle^* = a_1 \\ \langle\psi_2|\psi\rangle &= \langle\psi|\psi_2\rangle^* = a_2\end{aligned} \tag{1}$$

where $|a_1|^2 + |a_2|^2 = 1$, and we interpret $|a_1|^2$ and $|a_2|^2$ as the probabilities that the system is found to be in states $|\psi_1\rangle$ and $|\psi_2\rangle$, respectively. Generalization to superposition of an arbitrary number of states yields

$$|\psi\rangle = \sum_n a_n|\psi_n\rangle \tag{2}$$

$$\sum_n |a_n|^2 = 1 \tag{3}$$

with the interpretation that $|a_n|^2$ is the probability that the system is found to be in state $|\psi_n\rangle$.

In the classical model of optical communications, information can be incorporated in a laser beam by modulating

the amplitude, phase or polarization of the optical field. In the quantum model, information can be similarly incorporated into coherent states represented by the ket $|\alpha\rangle$ and described in great detail in [6]. Coherent states can be expressed as a superposition of orthonormal number states $|n\rangle$ as

$$|\alpha\rangle = e^{-\frac{1}{2}|\alpha|^2} \sum_{n=0}^{\infty} \frac{\alpha^n}{(n!)^{1/2}} |n\rangle \tag{4}$$

Coherent states are not orthogonal, as can be seen by considering the overlap of two arbitrary coherent states, $|\alpha\rangle$ and $|\beta\rangle$. Orthogonality requires that their overlap vanish, however for distinct coherent states the squared magnitude of their overlap is

$$|\langle\alpha|\beta\rangle|^2 = \left| e^{-(|\alpha|^2+|\beta|^2)/2} \sum_n \sum_m \frac{\alpha^n}{\sqrt{n!}} \frac{(\beta^*)^m}{\sqrt{m!}} \langle n|m\rangle \right|^2 \tag{5}$$
$$= \left| e^{(|\alpha|^2+|\beta|^2)/2} \sum_n \frac{(\alpha\beta^*)^n}{n!} \right|^2 = e^{|\alpha\ \beta|^2}$$

by virtue of the orthogonality of the number states $|n\rangle$. Equation (5) demonstrates that there is always some overlap between coherent states, regardless of how great the average photon count in each state may be [6, 7].

In the state-space interpretation of photon counting developed in [7], two signal states define a plane in Hilbert space. Application of the photon counting projection operators to the signal states generate "measurement states" [1] that span the two-dimensional subspace defined by the signal states, designated as $|w_0\rangle$ and $|w_1\rangle$ in Fig. 1. The squared magnitude of the projection of each signal state onto its associated measurement state is the probability that the signal state will be detected correctly. With this approach, the measurement state for the null hypothesis H_0, $|w_0\rangle$, is taken to be the ground state, corresponding to one of the two binary signals shown in Fig. 1a.

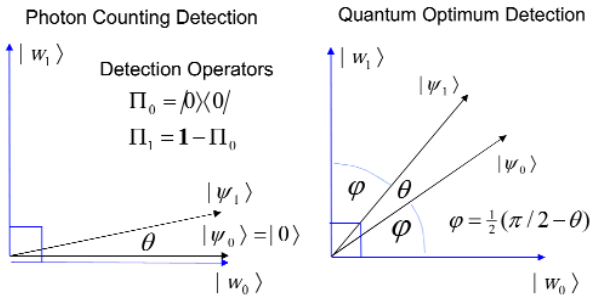

Fig. 1. Measurement state interpretation of binary coherent state detection: a) photon counting; b) optimum quantum measurement achieving the Helstrom bound.

The measurement state for the alternate hypothesis H_1, $|w_1\rangle$, does not in general align with any of the number states, but rather it is a superposition of number states except for the ground state, with coefficients determined by the signal state $|\psi_1\rangle$. A detailed description of this formulation is provided in [7]. The error probability is minimized and the Helstrom bound achieved when the two orthonormal measurement states are rotated symmetrically within the signal subspace, as shown in Fig. 1b. The resulting limit on the error probability has been derived in [7] by evaluating the signal-state projections onto each measurement state, and shown to be exactly equal the Helstrom bound:

$$P(E) = \tfrac{1}{2}\left(1 - \sqrt{1 - 4\,p_0 p_1\,|\langle\alpha|\beta\rangle|^2}\right) \tag{6}$$

The measurement-state approach therefore provides a geometrical interpretation of the optimum quantum measurement, which allows us to relate the abstract quantum optimum measurement to classical measurements that can be carried out in the laboratory.

III. NEAR-OPTIMUM DETECTION OF BPSK SIGNALS

Binary phase-shift keying (BPSK) modulation is particularly well suited to illustrating the key concepts in classical, near-optimum and optimum quantum detection strategies, as well as establishing a correspondence between classical and quantum receiver performance. An example of BPSK signaling is shown in Fig. 2: during each T-second symbol interval, the amplitude of the electric field is taken to be E if the binary data is "1", corresponding to hypothesis H_1, and $-E$ if the binary data is "0", corresponding to H_0. The signal amplitude therefore toggles between $\pm E$ in response to the data, but remains constant during each T-second symbol-interval. Assume that H_0 and H_1 occur with a priori probabilities p_0, p_1 respectively, where $p_0 + p_1 = 1$. The average photon-count within each received symbol interval is $K_\alpha = E^2T = |\alpha|^2$, while the actual photon-count is k. The quantum representation of the binary signals is $|-\alpha\rangle$ when H_0 is true, and $|\alpha\rangle$ when the alternate hypothesis, H_1, occurs.

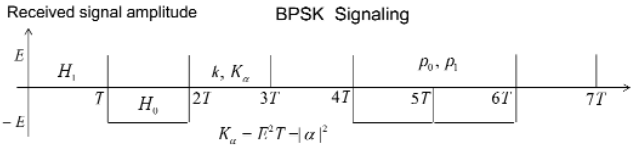

Fig. 2. Classical representation of binary phase-shift keyed (BPSK) data-stream.

For equal a priori probabilities, $p_0 = p_1$, the error probability for coherent detection of BPSK signals is given by the well-known expression $P(E) = \frac{1}{2}[1 - \mathrm{erf}(\sqrt{2K_\alpha})]$, where "erf" is the error function defined as $erf(x) = 2\pi^{-1/2}\int_0^x \exp(-t^2)dt$.

The Kennedy receiver

The displacement operator $D(\gamma)$ shifts any coherent state $|\alpha\rangle$ to a new coherent state $|\alpha+\gamma\rangle$, $D(\gamma)|\alpha\rangle = |\alpha+\gamma\rangle$. A near-optimum detection strategy for binary signals has been devised by R. S. Kennedy in 1974 [1]. The key idea of the Kennedy receiver is to apply the displacement operator $D(\alpha)$ to the coherent states $|-\alpha\rangle, |\alpha\rangle$ before photon-counting

detection, yielding $D(\alpha)|-\alpha\rangle=|0\rangle$ and $D(\alpha)|\alpha\rangle=|2\alpha\rangle$ for the two hypotheses, hence converting the phase-modulated BPSK signals in the classical representation to on-off-keyed signals, but with twice the amplitude and thus four times the pulse energy, since $|2\alpha|^2=4K_\alpha$.

The displaced states are detected using photon counting, yielding an average error probability $P(E)=\frac{1}{2}e^{-4K_\alpha}$ as shown below, corresponding to on-off-keyed signals with average pulse energy $4K_\alpha$. In terms of classical implementation, a constant phase-locked local laser field with amplitude E matched to the received field is first added to the signal using a beam-splitter, followed by conventional photon counting detection. The negative BPSK symbols with amplitude -E (corresponding to the null hypothesis H_0) are therefore converted to zero, whereas the positive symbols with amplitude E are converted to $2E$, as shown in Fig. 3. The detection strategy for the Kennedy receiver is: declare "H_1" if $k>0$, "H_0" if $k=0$.

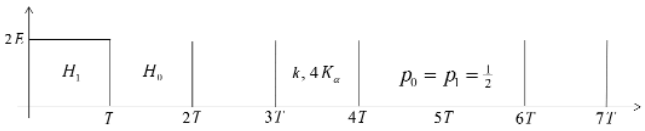

Fig. 3. BPSK signals converted to on-off keyed signals via the Kennedy detection strategy.

The relevant conditional probabilities are given by

$$H_0:\quad p(k=0)=1,\qquad H_1:\quad \begin{cases} p(k=0)=\exp(-4K_\alpha) \\ p(k>0)=1-\exp(-4K_\alpha) \end{cases}$$

$$P(E)=1-P(C)$$

The conditional probabilities of correct detection become $P(C|H_0)=1;\ P(C|H_1)=1-\exp(-4K_\alpha)$ which must be averaged over the a priories to obtain the average probability of correct detection: $P(C)=p_0P(C|H_0)+p_1P(C|H_1)$. With equal a priori probabilities the probability of correct detection is $P(C)\underset{p_0=p_1}{=}\frac{1}{2}\left(1+[1-\exp(-4K_\alpha)]\right)=1-\frac{1}{2}\exp(-4K_\alpha)$. The average error probability is related to the probability of correct detection as $P(E)=1-P(C)$, hence the average error probability of the Kennedy receiver is $P(E)\underset{p_0=p_1}{=}\frac{1}{2}\exp(-4K_\alpha)$.

Approaching the Helstrom bound via signal-state rotation

It is noteworthy that with the Kennedy receiver the cancelled signal always results in correct detection, since no photons can occur when there is no signal pulse. In addition, doubling the signal amplitude for the alternate hypothesis increases the signal energy by a factor of four, greatly reducing the probability of a zero photon-count when a pulse is present: these are the primary the reasons why the Kennedy receiver achieves near-optimum performance. However, photon-counting detection implies that one of the measurement states should be aligned with the ground state, and as we have seen, this is not the condition under which optimum performance is achieved. The state-space representation of optimum detection described in [7] and illustrated in Fig. 1b shows that the measurement states must be symmetrically arranged with the signal states for optimum detection, not asymmetrically as with photon-counting detection. It is therefore natural to ask under what conditions optimum detection could be approached by starting with photon-counting detection, and rotating the signal-states into a more symmetrical configuration with respect to the measurement states.

An approximate state-space representation of photon counting for small signal energies is shown in Fig. 4a, where the measurement states are approximated by the number states $|0\rangle$ and $|1\rangle$, so that $|w_0\rangle=|0\rangle$ and $|w_1\rangle=|1\rangle$. With photon-counting detection, the signal state representing H_0 is aligned with the measurement-state, resulting in $|\psi_0\rangle=|w_0\rangle=|0\rangle$, whereas the alternate state $|\psi_1\rangle$ is rotated in the $(|0\rangle,|1\rangle)$ plane by an angle θ related to the overlap of the signal-states as $\theta=\cos^{-1}(|\langle\psi_0|\psi_1\rangle|)=\cos^{-1}(e^{-\frac{1}{2}|2\alpha|^2})$: for example, with $|\alpha|=0.2$ the angle between the signal states is $\theta=22.6$ degrees.

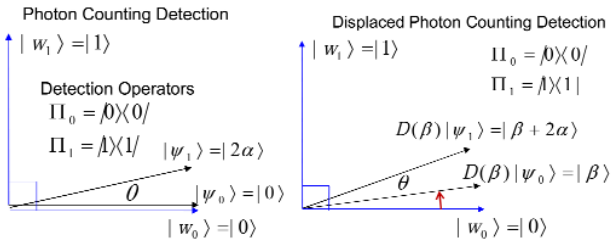

Fig. 4. Small signal energy representation of photon counting and displaced photon counting.

Recall from Fig. 1b that the measurement states should be placed symmetrically around the signal states in the signal subspace, the optimum rotation angle is $\varphi=\frac{1}{2}(\pi/2-\theta)$: for our example, the optimum rotation angle between the signal state $|\psi_0\rangle$ and its associated measurement state $|w_0\rangle$ should be $\varphi=33.7$ degrees, the same as between $|\psi_1\rangle$ and $|w_1\rangle$. From the overlap relation for coherent states, an angle of 33.7 degrees corresponds to an overlap of $\cos(33.7)=0.832=e^{-\frac{1}{2}|\beta|^2}$, yielding a displacement magnitude of $|\beta|=0.61$. This rotation can be accomplished by applying the displacement operator $D(\beta)$ to the signal states as indicated in Fig. 4b, where $|\beta|=0.61$ and $\arg(\beta)=\arg(\alpha)$. After displacement, the probability of finding $D(\beta)|\psi_0\rangle$ projected onto the next higher dimensional state $|2\rangle$, corresponding to a tilt in the signal subspace from the two-dimensional $(|0\rangle,|1\rangle)$ subspace into the three-dimensional $(|0\rangle,|1\rangle,|2\rangle)$ subspace, can be evaluated as $p(k=2)=|\langle 2|\beta\rangle|^2=|\beta|^4\ e^{-|\beta|^2}/2=0.04$. This is small enough to justify the two-dimensional measurement-state model, however this probability increases to

$|\langle 2|\beta+2\alpha\rangle|^2=0.183$ for $D(\beta)|\psi_1\rangle$, which is significantly greater than zero and hence cannot be ignored. Similarly, the probability of finding $D(\beta)|\psi_0\rangle$ projected onto any of the higher-dimensional states $|2\rangle,|3\rangle,\cdots$ is equal to the probability that it is not projected onto the states $|0\rangle$ or $|1\rangle$: $p(k\geq 2)=1-\sum_{k=0}^{1}|\langle k|\beta\rangle|^2$. These probabilities are shown in Fig. 5 as a function of $|\beta|$, from 0 to 1.

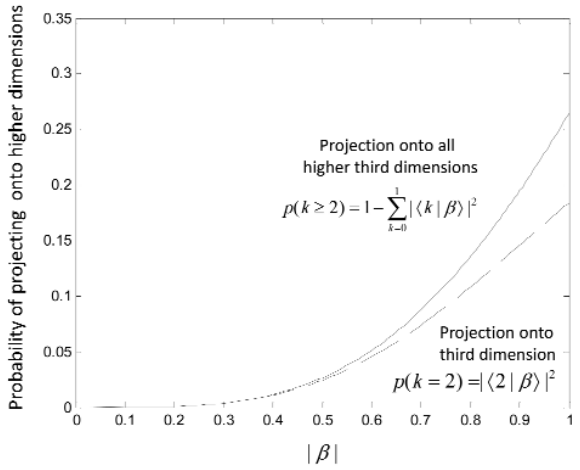

Fig. 5. Probability of finding a displaced ground state projected onto higher number state dimensions.

With the help of Fig. 5, we can argue that as long as the total displacement of the "pulse" state is less than approximately 0.2-0.3 in amplitude, the two-dimensional model should be accurate. For larger displacements, the projection onto third and higher dimensions starts to become significant, effectively tilting the signal subspace out of the two-dimensional $(|0\rangle,|1\rangle)$ subspace, hence the photon-counting interpretation is no longer accurate with larger displacements. This argument helps to explain why displacement followed by photon-counting detection approaches the optimum quantum measurement for small signal energies, but fails to reach it completely. However, the small-energy model still provides theoretical insights into the manner in which displacement followed by photon-counting detection approximates the Helstrom bound for small signal energies, and suggests approaches that may result in better receiver performance when small signal energies are involved.

The Optimized Kennedy Receiver

A displacement-optimized version of the Kennedy receiver, where the displacement does not cancel the null hypothesis exactly, but at the same time provides significant additional energy to the alternate, has been reported in [10], termed the "optimized displacement receiver". Here we provide an alternate derivation and interpretation of this idea. Since the displacement operator can be implemented with a strong local laser and a classical beamsplitter [9], the above discussion suggests that the performance of the Kennedy receiver could be improved in the small signal energy regime by first adding a phase-locked coherent field to the BPSK signals, detecting via photon-counting, then applying the optimum threshold defined in equation (7), which is valid for all displacements. The classical signal model for BPSK signals after displacement is shown in Fig. 6, where E_{LO} takes the place of the coherent state amplitude β.

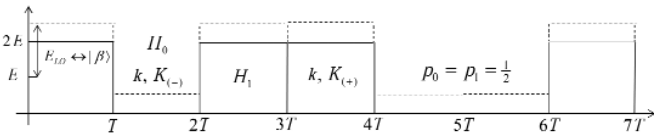

Fig. 6. Classical model of displaced BPSK signals, for the optimized Kennedy receiver.

The optimum value of the displacement for photon-counting detection can be derived by noting that for the small-energy region the value of the optimum threshold is always between 0 and 1. The goal of the optimization is to determine that value of β that maximizes the average probability of correct detection given β, $P(C)=\max_{\beta}P(C|\beta)$, or equivalently minimizes the average probability of error. With no loss in generality, assume that the signal amplitudes α,β are real, and write the conditional probabilities under the two hypotheses H_0 and H_1, given the displacement β, as $P(C|H_0,\beta)=\exp[-(\beta-\alpha)^2]$, $P(C|H_1,\beta)=1-\exp[-(\beta+\alpha)^2]$. Differentiating the conditional probability of correct detection, $P(C|\beta)=p_0P(C|H_0,\beta)+p_1P(C|H_1,\beta)$, with respect to β and solving the resulting transcendental equations numerically, the optimum displacement is that value of $\beta=\beta^*$ that satisfies the following transcendental equation as described in [10]: $p_0(\beta-\alpha)/p_1(\beta+\alpha)=\exp(-4\alpha\beta)$. This result is in contrast to the Kennedy receiver, where the signal fields are either cancelled completely or re-enforced by applying a displacement exactly equal to one of the signal amplitudes.

Applying the optimum displacement operator $D(\beta^*)$ to the binary signals results in the displaced signals $D(\beta^*)|-\alpha\rangle=|\beta^*-\alpha\rangle$ and $D(\beta^*)|\alpha\rangle=|\beta^*+\alpha\rangle$, with corresponding energies $|\beta^*-\alpha|^2=K_\alpha+K_\beta-2\sqrt{K_\alpha K_\beta}\equiv K_{(-)}$ and $|\beta^*+\alpha|^2=K_\alpha+K_\beta+2\sqrt{K_\alpha K_\beta}\equiv K_{(+)}$. It is easily shown that with displaced received fields and photon-counting detection the optimum threshold η is given by

$$\eta=\frac{\log_e(p_0/p_1)+4|\alpha||\beta|}{\log_e(|\beta+\alpha|^2/|\beta-\alpha|^2)} \qquad (7)$$

The optimum decision strategy calls for declaring H_1 if $k\geq\eta$, and H_0 if $k<\eta$. Note that non-zero counts are now possible even under H_0 due to the optimal displacement, unlike with the Kennedy receiver which displaced the signals sub-optimally by completely cancelling one of them. The relevant probabilities under the two hypotheses are given by

$$H_0: \quad p(k<\eta)=\sum_{k=0}^{\eta} K_{(-)}^k \exp(-K_{(-)})/k!$$

$$H_1: \begin{cases} p(k<\eta)=\sum_{k=0}^{\eta} K_{(+)}^k \exp(-K_{(+)})/k! \\ p(k\geq\eta)=1-\sum_{k=0}^{\eta} K_{(+)}^k \exp(-K_{(+)})/k! \end{cases}$$

For any signal energy, with optimal displacement the conditional probabilities of correct detection become $P(C\mid H_0)=p(k<\eta\mid K_{(-)});\ P(C\mid H_1)=1-p(k<\eta\mid K_{(+)})$, which must be averaged over the a priori probabilities to obtain the average probability of correct detection, finally yielding the average error probability as $P(E)=1-P(C)$. Due to the optimization of the displacement, these calculations are somewhat more involved than for the Kennedy receiver, as the following example illustrates.

Numerical Example

Consider the case $|\alpha|^2=0.2, |\alpha|=0.447$ with $p_0=p_1=\frac{1}{2}$. Solving the transcendental equation for β, we find the optimum displacement magnitude $|\beta|=0.757$ yielding the optimum threshold $\eta=0.86$ from equation (7). The conditional detection probability for the null hypothesis becomes $P(C\mid H_0)=p(k<\eta\mid K_{(-)})=\exp(-K_{(-)})=0.933$, whereas for the alternate hypothesis we obtain the following: $P(C\mid H_1)=1-p(k<\exp\eta\mid K_{(+)})=1-\exp(-K_{(+)})=0.765$. The average probability of correct detection follows directly as $P(C)=p_0P(C\mid H_0)+p_1P(C\mid H_1)=\frac{1}{2}(0.933+0.765)=0.849$, yielding $P(E)=1-P(C)=0.151$. This result is shown in Fig. 7 as the single point labeled "Numerical example" on the "Optimized Kennedy receiver" performance curve, which was computed numerically over the range of values $0<|\alpha|^2<0.8$. Note that the optimized Kennedy receiver described in [10] outperforms both the Kennedy and coherent receivers for all signal energies, including small signal energies where coherent detection actually approaches the Helstrom bound. However, it does not maintain this improvement over the Kennedy receiver for large symbol energies, but rather begins to approach the performance of the Kennedy receiver as the signal energy increases.

The above derivation suggests that by applying the optimum displacement to the BPSK signals prior to photon-counting detection, lower error probabilities will be obtained than possible with the Kennedy receiver, for any signal energy. The measurement-state derivation above also suggests that for the case of small signal energies, the Helstrom bound may be better approached by the optimized Kennedy receiver, since the displacement of the signal states is in the direction of the optimum measurement, where measurement states are placed symmetrically around the signal states in the $(|0\rangle,|1\rangle)$ plane.

As a heuristic check, we note that as the signal energy approaches zero the optimum displacement approaches $|\beta^*|^2=0.5$, or $|\beta|=0.707$ which now projects significantly onto higher number-state dimensions (as can be seen in Fig. 5, where the probability of projecting onto a higher dimension is seen to be 0.09). Hence the measurement-states no longer reside entirely in the $(|0\rangle,|1\rangle)$ plane, and the photon counting interpretation for displaced signal states is not strictly valid.

Nevertheless, displaced photon counting still approximates the optimum quantum measurement in this region, which explains why error probabilities close to the Helstrom bound can be achieved with the application of optimized displacement and photon-counting detection in this region.

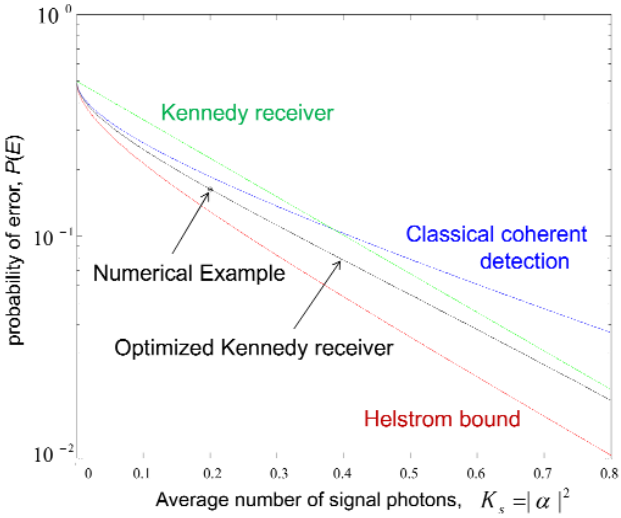

Fig. 7. Error probability performance of coherent, conventional Kennedy, and optimized Kennedy receivers.

Partitioned-Interval Detection Strategy

Consider the partitioned signal detection strategy illustrated in Fig. 8, where the original BPSK symbols have been converted to on-off signaling via matched displacement, as in the Kennedy receiver. Each T-second signal interval is now partitioned into two consecutive disjoint intervals: an initial interval of duration T_1 seconds, and a second interval of duration T_2 seconds. The average photon counts in these two intervals can be denoted as $4K_1$ and $4K_2$ respectively, with corresponding photon counts k_1 and k_2. The first interval is intended to be short, providing a small-energy (hence nearly quantum-optimum) "pre-detection" measurement, whereas the second interval is intended to supply more signal energy to further lower the error probability to acceptable levels for communication.

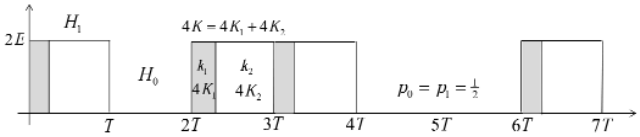

Fig. 8. Signal model for the partitioned interval detection strategy.

Based on the observation that for the Kennedy receiver correct detection occurs whenever the cancelled signal (null hypothesis) is observed, the strategy is to try to "guess" the correct hypothesis with a near-quantum-optimum measurement

in the first interval, and cancel the signal in the second interval by applying the appropriate displacement whenever a signal is pre-detected. If no signal is detected in the first interval, then the receiver continues to count photons in the second interval, without cancellation. This is similar to the approach used by the Dolinar receiver, which however must respond instantaneously to each photon-detection event within the signal interval, whereas here the counting intervals are determined based on predictable average signal energies instead of unpredictable photon occurrence times. Since with equal a priori probabilities roughly half of the original signal intervals contain no signal energy, it follows that any correct detection in the pre-detection interval will lead to more cancelled signals being observed in the second interval than in the original sequence. The final decision is based on the presence or absence of photon counts observed in the second interval, but also takes into account the outcome of the pre-detection measurement. The resulting two-step detection strategy can be summarized with the following algorithm:

If $k_1 > 0$, add 180° to the local field, and continue counting;
if $k_2 = 0$, decide "H_1"

If $k_1 = 0$, continue counting; if $k_2 > 0$, decide "H_1"
If $k_1 = 0$, continue counting; if $k_2 = 0$, decide "H_0"

This detection strategy is equivalent to a "modified sequence" interpretation, where some of the pulses in the second segment have been cancelled due to correct identification of the signal in the first segment. Restricting our attention to the second segment only, we find that this new sequence has more cancelled pulses than the original sequence where the a priori probabilities were equal. Therefore, if we observed only the modified sequence (where some of the original pulses have now been cancelled due to correct "pre-detection" decisions, but no new pulses have been added), then we would assign a higher probability to the occurrence of nulls in the second interval. Based on observing the modified sequence, we would conclude that the a priori probabilities p_0', p_1' of this new sequence were in fact not equal, but rather given by the expressions $p_0' = p_0 P(C|H_0) + p_1 P(C|H_1)$ and $p_1' = 1 - p_0'$. Representations of the modified sequence are shown in Fig. 9 a and b, where the intermediate decisions are shown in a) and the final sequence in b): for example, the second segment in the fourth symbol-interval ($3T < t \le 4T$) has been cancelled due to a correct decision in the first segment of this same interval, because a count $k_1 > 0$ has been observed in the first interval. The modified sequence therefore appears to have more null-hypotheses H_0' and fewer alternatives H_1'.

The decision strategy for the modified sequence shown in Fig. 9b, in terms of the modified a priori probabilities $p_0' > p_0$ and $p_1' < p_1$, can be stated as follows:

If $k_2 > 0$, declare H_1'; If $k_2 = 0$, declare H_0'.

However, now we must keep track of the correct decisions in the pre-detection segment that lead to pulse-cancellations, in order to detect the original message.

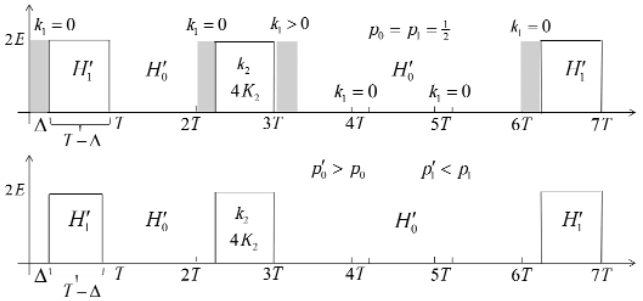

Fig. 9. a) Original and b) modified sequences, after a single correct pre-detection measurement.

We can now write the probability of correct detection and the probability of error for the modified sequence in terms of the modified a priori probabilities, as

$$\begin{aligned} P(C) &= p_0' P(C|H_0') + p_1' P(C|H_1') \\ &= (1-p_1') P(C|H_0') + p_1' P(C|H_1') \\ &= P(C|H_0') - p_1' [P(C|H_0') - P(C|H_1')] \end{aligned} \tag{8}$$
$$P(E) = 1 - P(C) = 1 - P(C|H_0') + p_1' [P(C|H_0') - P(C|H_1')]$$

Note that $P(C|H_0') \neq 1$ in general. Recalling that p_1' represents the probability of making an error in the first segment, and that the modified hypotheses $H_i'; i = 0,1$ refer to the second segment, we can see that the final error probability can always be improved by reducing p_1' if $P(C|H_0') > P(C|H_1')$, which is satisfied by the detection processes considered here, namely the Kennedy and optimized Kennedy receivers in the region of interest. Therefore, we can potentially choose a detection technique in the first segment that closely approaches the Helstrom bound for small signal energies, and perhaps a different detection strategy in the second segment, in order to achieve the desired error probability for communications applications. This result forms the basis of the "partitioned" approach, which we now examine for several cases of interest.

For the case of signal cancellation followed by photon-counting detection, the relevant probabilities for the modified sequence become

$$H_0': \quad p(k_2 = 0) = 1, \qquad H_1': \begin{cases} p(k_2 = 0) = \exp(-4K_2) \\ p(k_2 > 0) = 1 - \exp(-4K_2) \end{cases}$$

which yield the following conditional probabilities of correct detection: $P(C|H_0') = 1$, and for the alternate hypothesis $P(C|H_1') = 1 - \exp(-4K_2)$. Substituting into equation (8) yields $P(C) = p_0' + p_1'[1 - \exp(-4K_2)] = 1 - p_1' \exp(-4K)$, and error probability $P(E) = 1 - P(C) = p_1' \exp(-4K_2)$. Note that if $p_1' = \frac{1}{2}\exp(-4K_1)$, as would be obtained with photon-counting detection over the first segment, then the error probability after observing the entire symbol interval would

simply become $\frac{1}{2}\exp(-4K)$, which is exactly the same as for the Kennedy receiver, hence nothing would be gained. However, it also suggests that if $p_1' < \frac{1}{2}\exp(-4K_1)$ the error probability of the modified sequence will decrease correspondingly, resulting in $P(E) < \frac{1}{2}\exp(-4K)$. This observation provides a means for approaching the Helstrom bound by employing a better detection strategy in the first segment than simple field cancellation followed by photon counting detection, resulting in better overall performance. With $P_K(E)$, $P_c(E)$ and $P_{oK}(E)$ referring to the Kennedy, coherent and optimized Kennedy receivers respectively, the best strategy can be inferred from the ratio of the error probabilities $P_K(E)/P_c(E)$ and $P_K(E)/P_{oK}(E)$ in Fig. 10, which is interpreted as "gain over the Kennedy receiver". Note that in Fig. 10 N refers to the total number of segments used by the partitioned receiver, as explained subsequently in the section on the *Optimized N-segment receiver*.

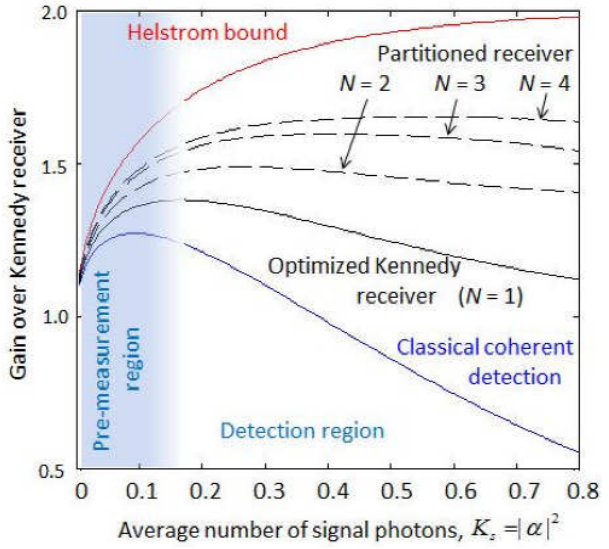

Fig. 10. Gain of coherent, optimized Kennedy, and partitioned receivers over the Kennedy receiver.

In Fig. 10, the coherent receiver peaks at $K_s = 0.095$ attaining a maximum gain of 1.272 over the Kennedy receiver, whereas the optimized Kennedy receiver peaks at $K_s = 0.165$, with a maximum gain of 1.381, after which both gains decrease: the gain of the optimized Kennedy receiver approaches 1 at high signal energies, reverting back to the conventional Kennedy receiver, whereas the gain of the coherent receiver continues to decrease towards zero.

Optimized N-segment receiver

The optimized two-segment detection approach described above can be extended directly to three or more segments, by considering the first N-1 segments of an N-segment receiver to be a "pre-detection" segment whose decision outcome modifies the a priori probabilities of the original sequence, thus improving the fidelity of the final decision. For example, the performance of a three-segment receiver can be evaluated by starting out as a two-segment receiver, but then partitioning the smaller pre-detection interval into two segments and optimizing each before optimizing the error probability for the third segment, further improving receiver performance. This procedure extends directly to an arbitrary number of segments, each step yielding an improvement over the previous step, but also increasing the complexity of the receiver.

The gain over the Kennedy receiver for up to four optimized segments reaches a maximum at slightly higher signal energies as can be seen in Fig. 10, which flatten out as the number of segments increase, effectively maintaining the maximum gain achieved by the pre-detection measurement over the region of interest. For three and four segment optimized receivers the maxima occur at $K_s = 0.38$ and $K_s = 0.62$ average signal photons. The gain curves can be divided roughly into two regions, a "pre-detection" region over which the gains increase rapidly, followed by a "detection" region over which the gains flatten out attempting to maintain maximum gain. The boundary between these two regions is roughly the initial small-energy region of up to approximately 0.2 signal photons, as shown in Fig. 10. This interpretation is in line with our previous conclusion that displacement followed by photon counting is close to the optimum strategy at small signal energies, hence we can interpret any measurement made within this region in a segmented receiver approach to be a pre-detection measurement: the use of multiple segments is merely a means to obtain better pre-detection performance. It should be noted that any other pre-detection strategy that improves upon these initial error probabilities will lead to gains in overall performance. Therefore, other measurement techniques that may be developed in the future could also be used to carry out pre-detection, potentially leading to further improvements in overall performance.

The error probability performance of optimized two, three and four segment receivers are shown in Fig. 11 along with that of the Kennedy receiver, coherent receiver and optimized Kennedy receiver for comparison. The partitioned receiver discussed here outperforms the previously known "near-optimum" approaches such as the Kennedy receiver for all signal energies, with gains of more than 2 dB over the Kennedy receiver at $P(E) = 0.1$, in the region of greatest interest for coded optical communications. This new approach effectively partitions the signal interval into two segments, a pre-detection segment that employs displaced photon counting to closely approach the Helstrom bound at small signal energies, followed by a detection segment that measures the remaining signal energy to achieve the desired communications performance.

For any number of predetermined segments N, the result of the first (N-1) decisions is incorporated into the probability of correct detection p_0' obtained from the first (N-1) segments, which is used as the a priori probability of hypothesis H_0' for the final segment. This strategy can be implemented using a bank of N lasers and switching between them using offset clocks operating at the symbol rate, hence it leads to practically implementable receivers for small values of N, but it also highlights the reason for suboptimal performance when

compared to the Dolinar receiver: since photons arrive randomly within any predetermined decision interval, the signal energy following a photon detection event in any sub-interval is effectively wasted with the partitioned-interval approach, since the contradicting decision could actually have be made as soon as the photon was detected.

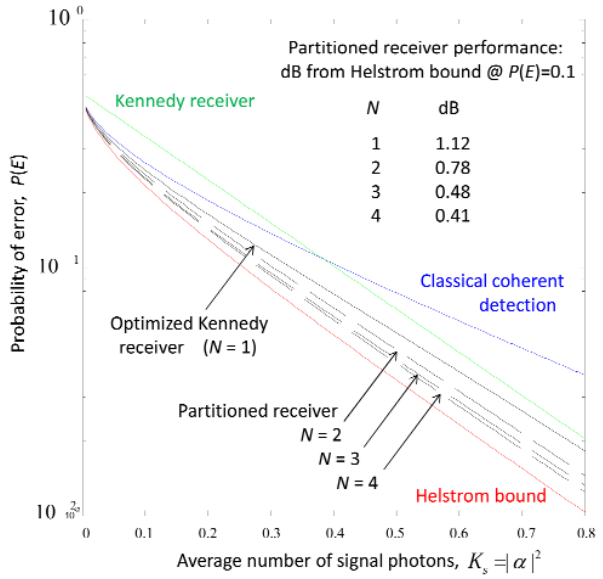

Fig. 11. Error probability performance and comparison of N-segment partitioned receivers.

However, responding instantly to each photon-occurrence requires processing bandwidth far exceeding the signal bandwidth, and hence leads to problems with implementation particularly at high data rates. This is one of the fundamental differences between the two approaches: the Dolinar receiver requires infinitely large processing bandwidths to reach the Helstrom bound, along with precisely controlled continuous-time laser intensities, whereas the partitioned-interval approach switches between a few local lasers with predetermined intensities at the signaling rate, but cannot approach the Helstrom bound arbitrarily closely for small, hence practical, values of N.

IV. Summary and Conclusions

An optical communications receiver concept capable of approaching the quantum limit in the region of interest for coded optical communications from deep-space, has been developed and analyzed in this paper. The key idea is to break up the signal interval into a short "pre-detection" segment followed by a longer validation segment in such a way as to optimize overall performance. This two-interval interpretation was extended to higher complexity N-interval detection by interpreting the processing in the first N-1 intervals as an improved pre-detection measurement, viewing the final N^{th} interval as the validation segment. It is shown that increasing N leads to improved performance for N = 2, 3, and 4 segments, arguably approaching the quantum limit for larger N but only at the cost of greater processing complexity. Therefore, this approach is intended primarily for low-complexity applications where improved receiver performance is deemed necessary. It was shown that with four disjoint segments, performance of the partitioned receiver approaches the Helstrom bound to within 0.41 dB, or equivalently improves upon the Kennedy receiver by 2 dB, at an error probability of 0.1 typically required by modern codes.

Acknowledgment

The research reported in this paper was carried out at the Jet Propulsion Laboratory, California Institute of Technology, under a contract with the National Aeronautics and Space Administration.

References

[1] C. W. Helstrom, Quantum Detection and Estimation Theory, Mathematics in Science and Engineering, Academic Press, New York, 1976.

[2] M. Sasaki, O. Hirota, "Optimum decision scheme with a unitary control process for binary quantum-state signals," Physical Review A, Volume 54, 1996.

[3] C.-W. Lau, V. A. Vilnrotter, S. Dolinar, J. M. Geremia, and H. Mabuchi, "Binary Quantum Receiver Concept Demonstration," Interplanetary Network Progress Report 42-165, Jet Propulsion Laboratory, May 15, 2006.

[4] R. Cook, P. Martin, J. M. Geremia, "Optical coherent state discrimination using a closed-loop quantum measurement," Nature, vol. 446, 12 April 2007.

[5] A. Acin, E. Bagan, M. Baig, L. Masanes, R. Munoz-Tapia, "Multiple-copy state discrimination with individual measurements," Physical Review A, Volume 71, 2005.

[6] R. J. Glauber, "Coherent and Incoherent States of the Radiation Field, The Physical review, vol. 123, no. 6, 1963.

[7] V. A. Vilnrotter, C-W. Lau, "Quantum Detection and Channel Capacity for Communications Applications," Proceedings of SPIE, Vol. 4635, 2002.

[8] S. M. Barnett, P. M. Radmore, Methods in Theoretical Quantum Optics, Oxford Series in Optical and Imaging Sciences, Clarendon Press, Oxford, 1997.

[9] M. Paris, "Displacement operator by beam splitter," Physics Letters A, Elsevier, 1996.

[10] C. Wittmann, M. Takeoka, K. Cassemiro, M. Sasaki, G. Leuchs, U. Andersen, "Demonstration of Near-Optimal Discrimination of Optical Coherent States," Physical Review Letters, vol. 101, 21 November 2008.

Victor A. Vilnrotter (M'79, SM'02) was born in Kúnhegyes, Hungary, in 1944. He received his Ph.D. in electrical engineering and communications theory from the University of Southern California in 1978 and joined the Jet Propulsion Laboratory, Pasadena, Calif., in 1979, where he is a Principal Engineer in the Communication Architectures and Research Section. His research interests include electronic compensation of large antennas with focal-plane arrays, adaptive combining algorithms for antenna arrays, optical communications through atmospheric turbulence, the application of quantum communications to deep-space optical links, and the development of uplink array calibration and tracking technologies. He has published extensively in conferences and refereed journals, and has received numerous NASA awards for technical innovations, and a NASA Exceptional Service Medal for contributions in signal processing.